SPANDIDOS PUBLICATIONS

ONCOLOGY LETTERS 23: 157, 2022

miR-31-5p-*DMD* axis as a novel biomarker for predicting the development and prognosis of sporadic early-onset colorectal cancer

CHANGQIN LIU[1], WEI WU[1], WENJU CHANG[2], RUIJIN WU[1], XIAOMIN SUN[1], HUILI WU[3] and ZHANJU LIU[1,3]

[1]Department of Gastroenterology, The Shanghai Tenth People's Hospital of Tongji University, Shanghai 200072; [2]Department of General Surgery, Zhongshan Hospital of Fudan University, Shanghai 200032; [3]Department of Gastroenterology, Zhengzhou Central Hospital Affiliated to Zhengzhou University, Zhengzhou, Henan 450007, P.R. China

Received October 23, 2021; Accepted February 9, 2022

DOI: 10.3892/ol.2022.13277

Abstract. The incidence of colorectal cancer (CRC) is increasing in young adults, but knowledge regarding the molecular features of sporadic early-onset colorectal cancer (SEOCRC) is limited. The objective of the present study was to investigate potential key tumorigenesis-associated genes and their regulatory microRNAs (miRNAs) in SEOCRC. Using miRNA and mRNA expression screening of SEOCRC and sporadic late-onset colorectal cancer (SLOCRC) by next generation sequencing (NGS) and bioinformatics, the SEOCRC-associated miRNAome and transcriptome were analyzed. In SEOCRC miRNA and mRNA expression profiles, the tumorigenesis-associated genes and their regulatory miRNAs were analyzed according to the miRTarBase database, and specific miRNA-mRNA pairs were selected as the candidate biomarkers in SEOCRC, which were further verified in another cohort of SEOCRC and SLOCRC patients' colon cancer and paracancerous tissues using reverse transcription-quantitative PCR and immunohistochemistry. Moreover, the clinical relevance of these paired signatures to clinicopathological features was determined in 80 patients with SEOCRC. The expression of dystrophin (*DMD*) was downregulated and that of miR-31-5p was upregulated in SEOCRC tissue compared with adjacent peritumoral tissue. While *DMD* and miR-31-5p were not differentially expressed in SLOCRC tissues compared with that in adjacent peritumoral tissues. The miR-31-5p-*DMD* axis was identified as the key regulatory axis specific to SEOCRC, and *DMD* expression was closely associated with TNM stage and lymph node metastasis. Importantly, Kaplan-Meier analysis revealed that patients with low *DMD* expression had significantly poorer overall survival, cancer specific survival and recurrence free survival compared with those with high expression of *DMD*. In conclusion, the miR-31-5p-*DMD* axis may serve as a novel biomarker in predicting the development of SEOCRC, and *DMD* can be used as a promising biomarker for the prognosis of SEOCRC.

Correspondence to: Dr Zhanju Liu, Department of Gastroenterology, The Shanghai Tenth People's Hospital of Tongji University, Building 2, 301 Yanchang Middle Road, Shanghai 200072, P.R. China
E-mail: liuzhanju88@126.com

Key words: sporadic early-onset colorectal cancer, sporadic late-onset colorectal cancer, microRNA-31-5p, dystrophin, prognosis

Introduction

Colorectal cancer (CRC) is one of the most frequently diagnosed malignancies and one of the leading causes of mortality worldwide (1). In 2018, there were >1.8 million new cases of CRC and 881,000 deaths worldwide, accounting for ~1 in 10 cancer cases and deaths (1). Overall, CRC ranked the third in incidence and the second in mortality (1). Currently, although the etiology and pathology are still not fully understood, it is generally considered that CRC is caused by multiple factors such as environmental factors, lifestyle, and genetic susceptibility (2). CRC may be caused by mutations that target oncogenes, tumor suppressor genes and genes related to DNA repair mechanisms (3). It can be classified as sporadic (70%), inherited (5%) or familial (25%) according to the origin of the mutation and the pathologies are classified into three types, chromosomal instability, microsatellite instability (MSI), and CpG island methylator phenotype. In these types of CRC, common mutations, as well as chromosomal changes and translocations have been reported to affect important pathways (such as MAPK/PI3K, WNT, TP53 and TGF-β signaling) (3). In addition to gene mutations, changes in long non-coding RNA or microRNA (miRNA/miR) are also found to be involved in different stages of carcinogenesis and may serve as predictive biomarkers (3).

The incidence of CRC has been rapidly rising in people <50 years old in the past 20 years (1,4). Moreover, early-onset colorectal cancer (EOCRC, <50 years old) differs from late-onset CRC (LOCRC, >50 years old) in numerous aspects, such as distinctive histological features, site of tumor location, stage at the presentation, and molecular profiles (5-7). Therefore, improved understanding the molecular mechanisms

of EOCRC may help the development of precise screening and therapeutic strategies.

EOCRC can be divided into two distinct subtypes, including the inherited subtype, which is a well-documented hereditary condition, and the sporadic subtype, which occurs without prior family history. Hereditary cases account for ~30% of EOCRC cases (8). The pathogenesis of the inherited subtype has been well characterized, and is mainly related to Lynch syndrome (9). A previous study has reported that 16% (72/450) of patients with EOCRC have gene mutations and that Lynch syndrome germline mutations in mismatch repair (MMR) genes, including MLH1, MSH2, MSH2/monoallelic MUTYH, MSH6 and PMS2, account for nearly 50% cases (37/72) (10). Moreover, another study using weighted gene co-expression network analysis has predicted that seven genes (*SPARC, DCN, FBN1, WWTR1, TAGLN, DDX28* and *CSDC2*) play an important role in the pathogenesis of EOCRC (11). However, the molecular features of sporadic EOCRC (SEOCRC) are still undefined.

In the present study, the mRNA and miRNA profiles of SEOCRC and sporadic LOCRC (SLOCRC) were analyzed using next-generation sequencing (Illumina HiSeq) and bioinformatics. Differentially expressed mRNAs and miRNAs in SEOCRC and SLOCRC were identified and validated using reverse transcription-quantitative PCR (RT-qPCR). The expression of the *DMD* gene was further examined using immunohistochemistry, and its clinical relevance to the prognosis was also evaluated.

Materials and methods

Patients and sample collection

Cohort 1. Between February and July 2019, 13 patients with primary CRC between 18 and 80 years old were recruited in the Shanghai Tenth People's Hospital of Tongji University (China), including 8 with SEOCRC (32-47 years, 4 males) and 5 with SLOCRC (60-72 years, 4 males). Tumor and pericarcinomatous tissues (5 cm away from visible tumor edges) were collected and stored at -80˚C until RNA isolation. The pathological stage was defined according to the UICC/AJCC TNM classification system (https://www.uicc.org/resources/tnm). Details are shown in Table I.

Cohort 2. The present study also selected the mRNA and miRNA data of 74 tumor tissues (31-49 years; 33 males, 41 females) and 3 pericarcinomatous tissues (41-48 years; all females) from different patients with EOCRC, and 531 tumor tissues (50-90 years, 286 males, 245 females) and 8 pericarcinomatous tissues (54-90 years; 2 males, 6 females) from different patients with LOCRC from the Cancer Genome Atlas (TCGA) database (https://portal.gdc.cancer.gov/) which is publicly available.

Cohort 3. Between July and December 2019, paired specimens of 13 tumors and 13 paracancerous SEOCRC tissue samples (33-48 years; 8 males), as well as 11 tumor and 11 SLOCRC paracancerous tissue samples (53-79 years; 7 males) were collected in the Shanghai Tenth People's Hospital of Tongji University. For each patient, one tissue section was stored at -80˚C for RNA isolation and another tissue section was embedded in paraffin for immunohistochemistry.

Cohort 4. Surgical specimens of sporadic CRC tissues and adjacent normal tissues were obtained from patients with a diagnosis of primary SEOCRC who underwent surgery in the Shanghai Tenth People's Hospital of Tongji University between January 2011 and December 2015. None of the patients had received radiotherapy before surgery excision. A total of 80 tissue samples (30-48 years, 47 males) were immediately frozen in liquid nitrogen and stored at -80˚C until further use.

The diagnosis of all patients was confirmed by colonoscopy and pathology. Inherited cases and patients who received radiotherapy or chemotherapy before surgery or colonoscopy were all excluded. Informed written consent was obtained from all patients, and the study was approved by the Ethics Committee of the Shanghai Tenth People's Hospital, Tongji University.

RNA isolation. RNA was isolated from tumor and pericarcinomatous tissues using TriReagent (Ambion Inc.). Agarose gel electrophoresis was performed to determine the extent of RNA degradation and contamination, and the purity of the RNA was also measured by Nanodrop (ND-1000). The concentration was precisely quantified using a Qubit3 (Thermo Fisher Scientific, Inc.), and the integrity was measured using an Agilent 2100 Bioanalyzer (Agilent Technologies, Inc.). Samples with a RIN value of 7 and above were used for further analysis.

RNA sequencing (RNAseq). The RNA-seq transcriptome library was prepared using 1 μg total RNA by TruSeq RNA sample preparation kit (cat. no. RS-122-2001; Illumina, Inc.) according to the manufacturer's instructions. Libraries were size-selected for cDNA target fragments of 300 bp on 2% Low Range Ultra Agarose followed by PCR amplification using Phusion DNA polymerase (New England Biolabs) for 15 PCR cycles. After quantification using a Qubit3, the paired-end RNA-seq sequencing library was sequenced using the HiSeq X Ten Reagent Kit v2.5 (cat. no. FC-501-2501; Illumina, Inc.) with the Illumina HiSeq Xten (2x150 bp read length) system.

Small RNA sequencing. Small RNA sequencing libraries were created using 1 μg total RNA according to the TruSeq small RNA sample Preparation kit (cat. no. RS-200-0048; Illumina, Inc.). Reverse transcription was performed to generate cDNA libraries and PCR was used to amplify and add unique index sequences to each library. After quantification using a Qubit3, the small RNA sequencing library was sequenced using HiSeq X Ten Reagent kit v2.5 (cat. no. FC-501-2501; Illumina, Inc.) with the Illumina HiSeq X Ten system.

Identification of differentially expressed genes (DEGs). The raw paired end reads were trimmed and quality-controlled using SeqPrep (v1.3.2-4; https://github.com/jstjohn/SeqPrep) and Sickle (https://github.com/najoshi/sickle) with default parameters. Subsequently, clean reads were separately aligned to the reference genome (hg19) using HISAT2 (v2.1.0; http://ccb.jhu.edu/software/hisat2/index.shtml) software. The mapped reads of each sample were assembled using StringTie (v2.0.5; https://ccb.jhu.edu/software/stringtie/ index.shtml) with a reference-based approach as described previously (12). Differential expression analysis was performed for the RNA-seq data using the edgeR v3.26.8 in R v3.6.0 with false

Table I. Histopathological characteristics of the patients with SEOCRC and SLOCRC.

Patient	Age, years	Sex	Location of tumor	Dimensions, cm	TNM staging	UICC staging	Dukes' staging	MAC staging
Early 1	47	Female	Sigmoid colon	6x4.5x1.5	T4aN0M0	IIB	B	B2
Early 2	33	Male	Sigmoid colon	5x4.5	T3N2bM0	IIIC	C	C2
Early 3	43	Male	Ascending colon	4x2x2	T1N0M0	I	A	A
Early 4	32	Female	Rectum	3x2x1	T1N1aM0	IIIA	C	C1
Early 5	37	Female	Transverse colon	6x4.5x1.1	T4aN1aMO	IIIB	C	C2
Early 6	46	Female	Ascending colon	4x2	T4aN1Am0	IIIB	C	C2
Early 7	46	Male	Sigmoid colon	11x10x8	T3N0M0	IIA	B	B2
Early 8	42	Male	Sigmoid colon	2x2	T3N2aM1a	IVA	-	-
Late 1	60	Male	Rectum	1.8x1.6x0.8	T1N0M0	I	A	A
Late 2	61	Male	Sigmoid colon	5x4x1	T3N0M0	IIA	B	B2
Late 3	64	Male	Transverse colon	6.5x3.5	T3N0M0	IIA	B	B2
Late 4	60	Male	Rectum	6x4.5x1	T4aN0M0	IIB	B	B2
Late 5	72	Female	Rectum	6x3	T3N0M0	IIA	B	B2

Early: Tumor tissue from patients with SEOCRC. Late: Tumor tissue from patients with SLOCRC. The data were obtained from Cohort 1. SEOCRC, sporadic early-onset colorectal cancer; SLOCRC, sporadic late-onset colorectal cancer; UICC, Union for International Cancer Control; MAC, Modified Astler Coller.

discovery rate (FDR) correction (13,14). The genes that met the conditions of $\log_2$ fold-change ($\log_2$FC) >2 (where FC is the fold change in expression) and P<0.01 were considered to be differentially expressed.

Identification of differentially expressed miRNAs (DEMs). FASTX-Toolkit (v0.0.13; http://hannonlab.cshl.edu/fastx_toolkit/) was used to cut all small RNA sequencing reads at the 3' end to remove the adapter sequences. After adaptor trimming, reads were aligned to the human genome build 19 (hg19) using BLAST 2.10.1 (http://blast.ncbi.nlm.nih.gov/). The number of reads with each known microRNA from miRBase v22 was counted using mirdeep2 (https://drmirdeep.github.io/mirdeep2_tutorial.html). DEMs were obtained using edgeR package using log2 fold-change ($\log_2$FC) >2 and P<0.01 as cut-offs.

Prediction of regulatory miRNAs of DEGs. According to the recognition mechanism of miRNAs and mRNAs, the DEM and DEG pairs were selected in SEOCRC by bioinformatics analysis using miRTarBase database 8.0 (http://mirtarbase.mbc. nctu.edu.tw/).

miRNA extraction and RT-qPCR. To determine miRNA levels, total RNA of colon tissue (cohort 3) was isolated with the miRcute miRNA Isolation Kit (Tiangen Biotech Co., Ltd.) according to the manufacturer's protocol. miRNA was reverse transcribed into cDNA using a miRcute miRNA First-Strand cDNA Synthesis Kit (Tiangen Biotech Co., Ltd.) at 37˚C for 60 min. A miRcute miRNA qPCR Detection Kit (SYBR Green; Tiangen Biotech Co., Ltd.) was used for RT-qPCR analysis on an ABI 7500 fast real-time PCR system (Applied Biosystems) following the manufacturer's instructions. The cDNA (1 μl) was added to a 10-μl reaction system for amplification at 94˚C for 2 min; followed by 42 cycles of 94˚C for 20 sec and 60˚C for 34 sec. All reactions were performed in triplicate. The specificity of the qPCR product was confirmed using melting curve analysis, and miRNAs with a Cq value >35 and a detection rate <75% in each group were excluded from further analysis. The relative expression of miRNA was normalized to that of the internal control U6. Relative expression was calculated using the $2^{-\Delta\Delta Cq}$ method (15). The sequences of the forward primers are shown in Table II. Universal Reverse primers were obtained from Tiangen Biotech Co., Ltd.

RNA extraction and RT-qPCR. RNA was extracted from tissue samples (cohort 3 and 4) using the conventional TRIzol® (Invitrogen; Thermo Fisher Scientific, Inc.) method. Up to 1 μg total RNA was reversed transcribed into cDNA using the cDNA synthesis kit (Takara Bio, Inc.). The reaction conditions were 37˚C for 15 min and 85˚C for 5 sec. The following primer pairs were used: *DMD* forward, 5'-TGG GCAAACTGTATTCACTCAAAC-3' and reverse, 5'-TTC CCTTGTGGTCACCGTAGT-3'; GAPDH forward, 5'-GGA GCGAGATCCCTCCAAAAT-3' and reverse, 5'-GGCTGT TGTCATACTTCTCATGG-3'. qPCR assays were performed using SYBR Green qRT-PCR kits (Takara Bio, Inc.). For each sample, 10-μl reactions were set up containing 5 μl SYBR Premix, 0.2 μl ROX-2, 0.2 μl forward primer (10 μM/μl), 0.2 μl reverse primer (10 μM/μl), 1 μl cDNA, 3.4 μl ddH_2O. All PCR reactions were performed in triplicate. The following cycling protocol was used: 95˚C for 30 sec, followed by 40 cycles of 95˚C for 5 sec and 60˚C for 30 sec. The relative expression levels for the target gene were calculated using the $2^{-\Delta\Delta Cq}$ method (15).

Immunohistochemistry. Immunohistochemical (IHC) staining was performed on 4-μm sections of paraffin-embedded tissue samples to detect the expression levels of DMD protein from patients in Cohort 3. Paraffin-embedded tissue sections were

Table II. Forward primers used for reverse transcription-quantitative PCR analysis of cohort 2.

Gene name	Sequence (5'-3')
hsa-mir-9-3p	ATAAAGCTAGATAACCGAAAGT
hsa-mir-10b-5p	TACCCTGTAGAACCGAATTTGTG
hsa-mir-31-3p	TGCTATGCCAACATATTGCCAT
hsa-mir-31-5p	AGGCAAGATGCTGGCATAGCT
hsa-mir-34b-3p	CAATCACTAACTCCACTGCCAT
hsa-mir-101-5p	CAGTTATCACAGTGCTGATGCT
hsa-mir-204-5p	TTCCCTTTGTCATCCTATGCCT
hsa-mir-206	TGGAATGTAAGGAAGTGTGTGG
hsa-mir-592	TTGTGTCAATATGCGATGATGT
U6	CGCAAGGATGACACGCAAATTCGT

A universal reverse primer was used (cat. no. FP401-02; Tiangen Biotech Co., Ltd.). hsa, *Homo sapiens*; mir, microRNA.

mounted on glass slides and heated for 30 min at 55˚C. Then they were dewaxed three times in xylene for 10 min each time, followed by rehydration: 100% ethanol twice for 5 min each time, 90% ethanol for 5 min, 70% ethanol for 5 min, ddH_2O for 5 min. H_2O_2 solution (3%) was used to block endogenous peroxidase activity for 10 min at 37˚C and phosphate-buffered saline (PBS; Thermo Fisher Scientific, Inc.) was used to wash the slides twice for 5 min each time. The sections were immersed in 0.01 mmol/l sodium citrate buffer solution (pH 6.0; Thermo Fisher Scientific, Inc.) and incubated at 100˚C for 20 min and then they were rinsed twice with PBS (Thermo Fisher Scientific, Inc.) for 5 min each time. After incubation with 5% normal goat serum (Thermo Fisher Scientific, Inc.) for 20 min at 37˚C, these sections were then incubated with anti-human DMD monoclonal antibody (Abcam; catalog no. ab15277; dilution 1:200) at 4˚C overnight. After washing, the sections were incubated for 60 min with HRP-conjugated goat anti-Rabbit IgG (Abcam; catalog no. ab150077; dilution 1:400) at room temperature. The color reaction was developed with 3,3'-diaminobenzidine and the sections were counterstained with hematoxylin at room temperature for 30 sec followed by rinsing with distilled water for 30 min. Then the slides were dehydrated as follows: 70% ethanol dehydration for 3 min, 80% ethanol for 3 min, 95% ethanol for 3 min, 95% ethanol for 3 min, anhydrous ethanol for 3 min and xylene for 3 min. A light Leica microscope was used at x100 and x200 magnification (Leica Microsystems GmbH).

Statistical analysis. The GraphPad prism 5.0 software (GraphPad software, Inc.) was used for statistical analysis. According to whether the data are normally distributed, the RT-qPCR results were analyzed with paired t-test or Wilcoxon's signed rank tests. The association between the clinicopathological characteristics of the patients and *DMD* expression was analyzed using Fisher's exact test. The survival curves were plotted according to the Kaplan-Meier method, and the log-rank test was used for their statistical analysis. $P<0.05$ was considered to indicate a statistically significant difference.

Results

Expression profiles of DEGs in SEOCRC and SLOCRC. In the present study, 13 patients with CRC were enrolled and divided into SEOCRC (<50 years; n=8) and SLOCRC (≥50 years; n=5) groups (cohort 1). A total of 1,589 DEGs were identified between the tumor (n=8) and pericarcinomatous tissues (n=7; one samples was excluded to poor RNA quality) of patients with SEOCRC, including 913 upregulated genes and 676 downregulated genes (Fig. 1A). In SLOCRC, 1,383 DEGs were identified between tumor and pericarcinomatous tissues (n=5 each), including 481 upregulated genes and 902 downregulated genes (Fig. 1B). By comparing the DEGs between SEOCRC and SLOCRC, 837 DEGs were found only in SEOCRC and 631 DEGs only in SLOCRC (Fig. 1C and D).

To confirm these results, TCGA datasets were analyzed. In the TCGA group (cohort 2), a differential analysis was performed based on mRNA profiling data of 74 cases with CRC and 3 pericarcinomatous normal control tissues of EOCRC that were extracted from TCGA data portal. In total, 655 DEGs were identified, including 150 upregulated genes and 505 downregulated genes. Similarly, 1586 DEGs were identified between 531 cancer tissues and 8 pericarcinomatous tissue samples of LOCRC, including 712 upregulated genes and 874 downregulated genes. Among the 655 and 1586 DEGs, 125 DEGs were specific to EOCRC and 1,056 DEGs were specific to LOCRC, respectively (Fig. 1E).

By combining the results of these two mRNA profiling studies, *DMD* and *MPPED2* were identified (Table III) as the signature genes in the EOCRC group, consistent with a previous report showing *MPPED2* as a hypermethylated biomarker of CRC (16). Taken together, these results indicated that the molecular mechanism of SEOCRC is different from that in SLOCRC and that *DMD* and *MPPED2* may play a role in the onset of SEOCRC.

Expression profiles of DEMs in SEOCRC & SLOCRC. In the experimental group, 116 DEMs were identified between 8 tumor and 7 pericarcinomatous tissue samples of SEOCRC, including 68 upregulated and 48 downregulated miRNAs (Fig. 2A). 99 DEMs were identified between 5 cancer tissues and 5 pericarcinomatous tissues of SLOCRC, including 25 upregulated and 74 downregulated miRNAs (Fig. 2B). Among these DEMs, 78 DEMs were specific to EOCRC while 61 DEMs were specific to LOCRC (Fig. 2C).

In TCGA group (cohort 2), a differential analysis was also carried out based on miRNA profiling data of 74 CRC cases and 3 pericarcinomatous tissue samples from patients of EOCRC from TCGA. In total, 217 DEMs were identified, including 137 upregulated miRNAs and 80 downregulated miRNAs. Similarly, 325 DEMs were identified between 531 cancer and 8 pericarcinomatous tissues samples from patients with LOCRC, including 198 upregulated miRNAs and 127 down-regulated miRNAs. Among these DEMs, 22 DEMs were specific to EOCRC while 130 DEMs were specific to LOCRC (Fig. 2D).

By combining the results of these two miRNA profiling studies, miR-31-5p and miR-31-3p were identified as the distinctive miRNAs in the EOCRC group (Table IV), which has previously been reported to be associated with

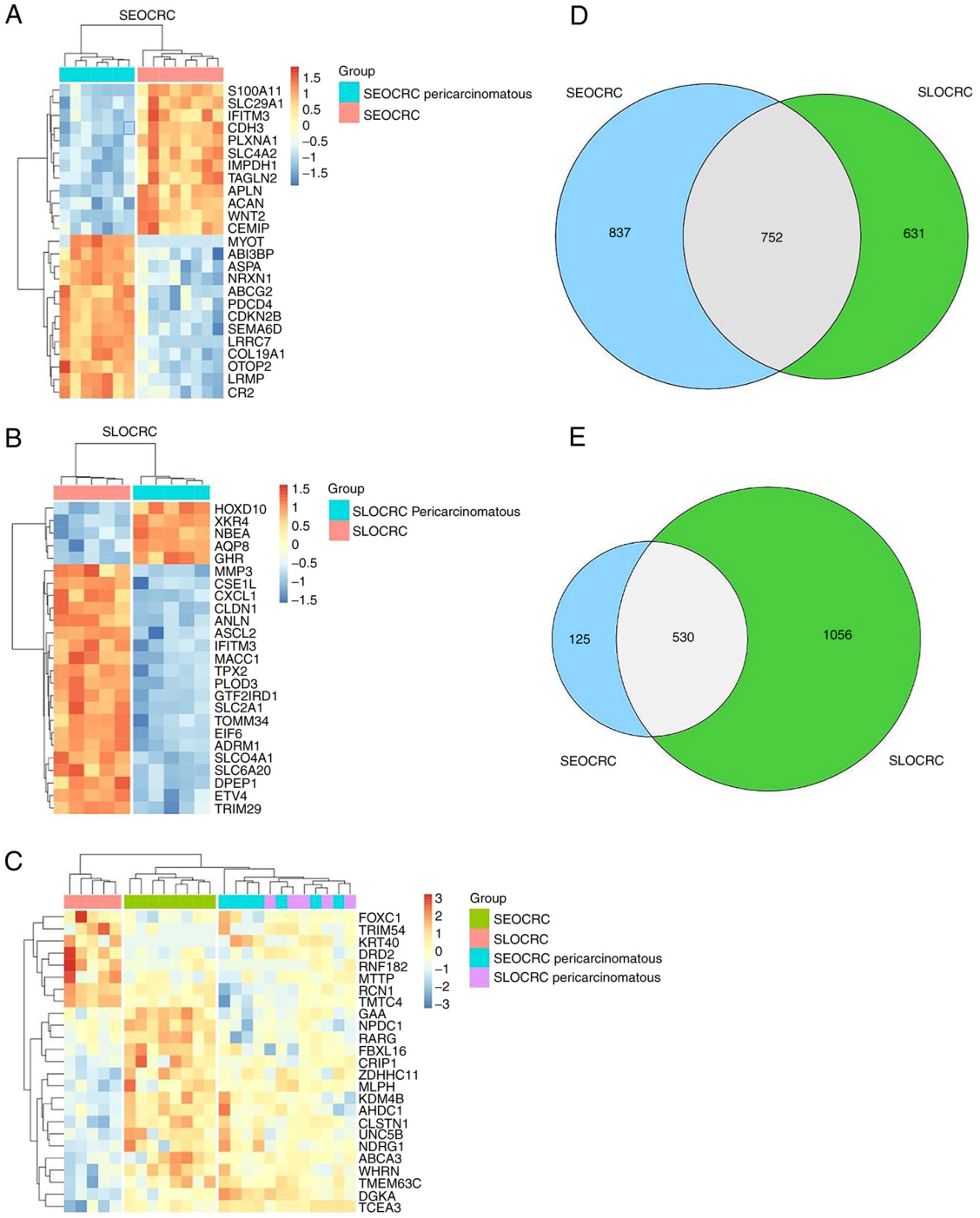

Figure 1. Identification of DEGs in SEOCRC and SLOCRC. (A) Heatmap of the top 25 DEGs in SEOCRC tissues compared with pericarcinomatous tissue. (B) Heatmap of the top 25 DEGs in SLOCRC tissues compared with pericarcinomatous tissue. (C) Heatmap of the top 25 DEGs in SEOCRC tissues compared with SLOCRC. (D) Venn diagram showing 837 DEGs unique to SEOCRC and 631 unique to SLOCRC of experimental group. The data were obtained from Cohort 1. (E) Venn diagram showing 125 DEGs unique to SEOCRC and 1,056 unique to SLOCRC of TCGA group. The data were obtained from Cohort 2. SEOCRC, sporadic early-onset colorectal cancer; SLOCRC, sporadic late-onset colorectal cancer; DEG, differentially expressed gene.

CRC (17-21). Taken together, these results further indicated that the molecular mechanism of SEOCRC is different from that of SLOCRC and that miR-31-5p and miR-31-3p may take part in the pathogenesis of SEOCRC.

Identification of key tumor-related genes and their regulatory miRNAs in SEOCRC. All SEOCRC private DEGs and DEMs in the experimental (cohort 1) and the TCGA (cohort 2) groups were matched using miRTarBase database. There were 10 DEMs and DEGs matched pairs in the experimental group including *CDK4* with miR-34b-3p, *DMD* with miR-31-5p, *DMD* with miR-9-3p, *TFAP2C* with miR-10b-5p, *NECTIN4* with miR-31-3p, *IGFBP2* with miR-204-5p, *SOX9* with miR-206, *SOX9* with miR-101-5p, *SOX9* with miR-592 and *CSMD1* with miR-10b-5p. Moreover, there were 2 DEGs and DEMs pairs in the TCGA group, including *DMD* with miR-31-5p and *SOX4* with miR-31-5p. Interestingly, *DMD* was observed to be downregulated while miR-31-5p was upregulated in both

Table III. DEGs specific to SEOCRC were shared by the experimental group and the TCGA group.

Group	Gene	Log_2 FC	P-value	FDR	Expression
Experimental group	DMD	-2.769013037	$1.37x10^{-10}$	$1.43x10^{-8}$	Downregulated
Experimental group	MPPED2	-3.151889779	0.002553869	0.009940859	Downregulated
TCGA group	DMD	-2.188531129	0.000134702	0.003064467	Downregulated
TCGA group	MPPED2	-2.054712209	0.000520196	0.00879555	Downregulated

The data were obtained from Cohort 1. hsa, *Homo sapiens*; miR, microRNA; DEG, differentially expressed gene; DEM, differentially expressed microRNA; SEOCRC, sporadic early-onset colorectal cancer; FC, fold change; FDR, false discovery rate.

Table IV. DEMs specific to SEOCRC were shared by the experimental group and the TCGA group.

Group	Gene	Log FC	P-value	FDR	Type
Experimental group	hsa-miR-31-5p	3.43133174	0.001694065	0.018612422	Upregulated
Experimental group	hsa-miR-31-3p	6.375239183	0.001308524	0.017072145	Upregulated
TCGA group	hsa-miR-31	5.590640822	0.003093682	0.009872114	Upregulated

The data were obtained from Cohort 1. hsa, *Homo sapiens*; miR, microRNA; DEG, differentially expressed gene; DEM, differentially expressed microRNA; SEOCRC, sporadic early-onset colorectal cancer; FC, fold change; FDR, false discovery rate.

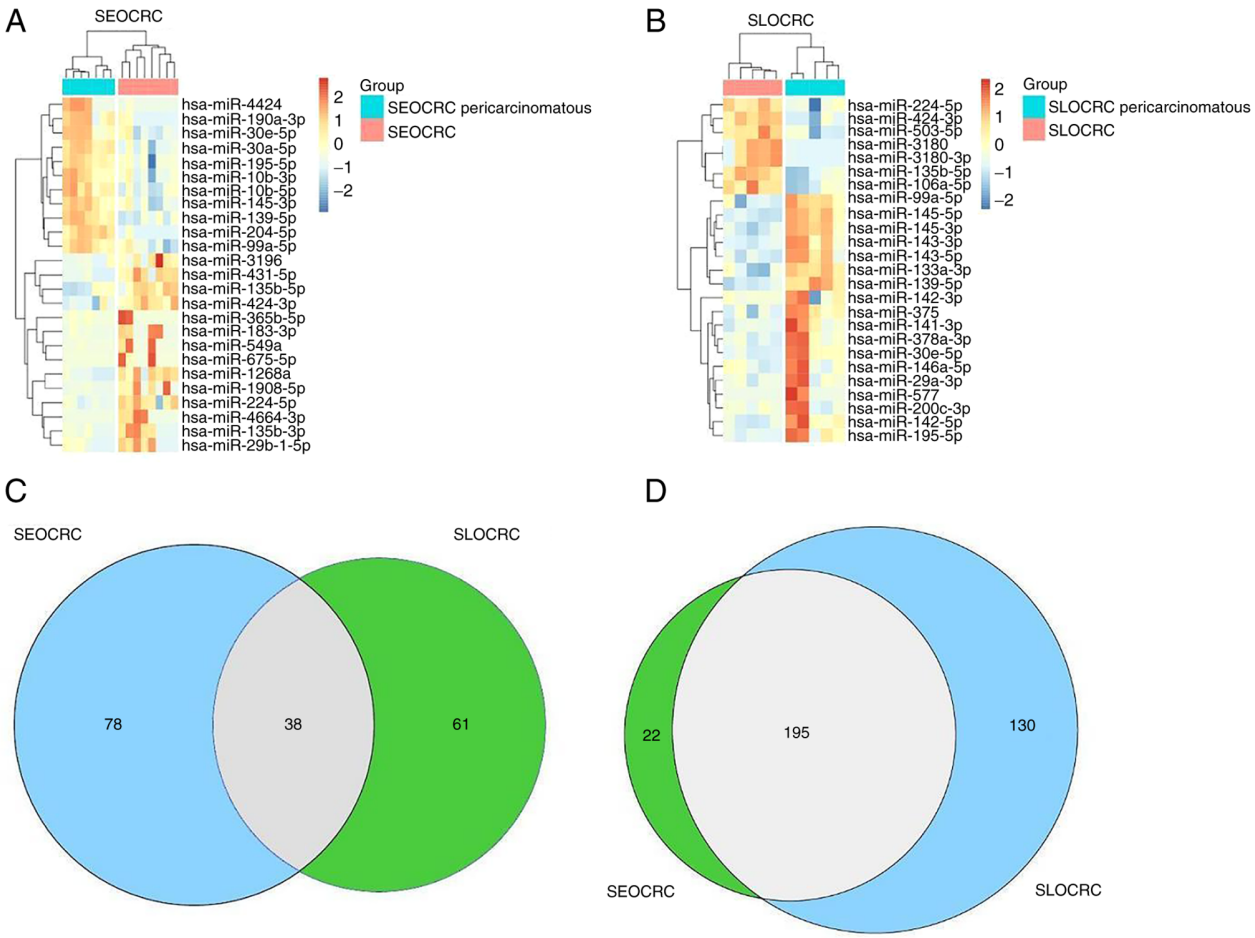

Figure 2. Identification of DEMs in SEOCRC and SLOCRC. (A) Heatmap of the top 25 DEMs in SEOCRC tissue compared with pericarcinomatous tissue. (B) Heatmap of the top 25 DEMs in SLOCRC compared with pericarcinomatous tissue. (C) Venn diagram showing 78 DEMs unique to SEOCRC and 61 unique to SLOCRC of experimental group. The data were obtained from Cohort 1. (D) Venn diagram showing 22 DEMs unique to SEOCRC and 130 unique to SLOCRC in TCGA data. The data were obtained from Cohort 2. SEOCRC, sporadic early-onset colorectal cancer; SLOCRC, sporadic late-onset colorectal cancer; DEM, differentially expressed microRNA.

Table V. Key DEGs and paired DEMs identified in SEOCRC.

A, TCGA group

First author, year	miRTarBase ID	miRNA	Target gene	Target Entrez Gene ID	Experiments	Support type	(Refs.)
Cacchiarelli *et al*, 2011	MIRT005456[a]	hsa-miR-31-5p	DMD	1756	Luciferase reporter assay, RT-qPCR, western blotting	Functional MTIs	(22)
Koumangoye *et al*, 2015	MIRT733212	hsa-miR-31-5p	SOX4	6659	Chromatin immunoprecipitation, immunoprecipitation, RT-qPCR, western blotting	Functional MTIs	(23)

B, Experimental group

First author, year	miRTarBase ID	miRNA	Target gene	Target gene Gene ID	Experiments	Support type	(Refs.)
Suzuki *et al*, 2010	MIRT003450	hsa-miR-34b-3p	CDK4	1019	Microarray, western blotting, RT-qPCR	Functional MTIs	(24)
Cacchiarelli *et al*, 2011	MIRT005456[a]	hsa-miR-31-5p	DMD	1756	Luciferase reporter assay, RT-qPCR, western blotting	Functional MTIs	(22)
Gabriely *et al*, 2011	MIRT006367	hsa-miR-10b-5p	TFAP2C	7022	Luciferase reporter assay, western blotting	Functional MTIs	(25)
Geekiyanage *et al*, 2016	MIRT731898	hsa-miR-31-3p	NECTIN4	81607	Luciferase reporter assay, western blotting	Functional MTIs	(26)
Chen *et al*, 2016	MIRT732358	hsa-miR-204-5p	IGFBP2	3485	Western blotting, luciferase reporter assay, microarray, RT-qPCR	Functional MTIs	(27)
Sim *et al*, 2016	MIRT733192	hsa-miR-9-3p	DMD	1756	Luciferase reporter assay	Functional MTIs	(28)
Zhang *et al*, 2015	MIRT733693	hsa-miR-206	SOX9	6662	Luciferase reporter assay, western blotting	Functional MTIs	(29)
Liu *et al*, 2017	MIRT734338	hsa-miR-101-5p	SOX9	6662	Luciferase reporter assay, RT-qPCR, western blotting	Functional MTIs	(30)
Zhu *et al*, 2016	MIRT734672	hsa-miR-10b-5p	CSMD1	64478	Immunocytochemistry, immunohistochemistry, luciferase reporter assay, RT-qPCR	Functional MTIs	(31)

[a]Indicates the DEM-DEG pairs that are shared between the experimental group and the TCGA dataset. The data were obtained from Cohort 1. hsa, *Homo sapiens*; miR, microRNA; DEG, differentially expressed gene; DEM, differentially expressed microRNA; SEOCRC, sporadic early-onset colorectal cancer; MTI, miRNA-target interaction; RT-qPCR, reverse transcription-quantitative PCR.

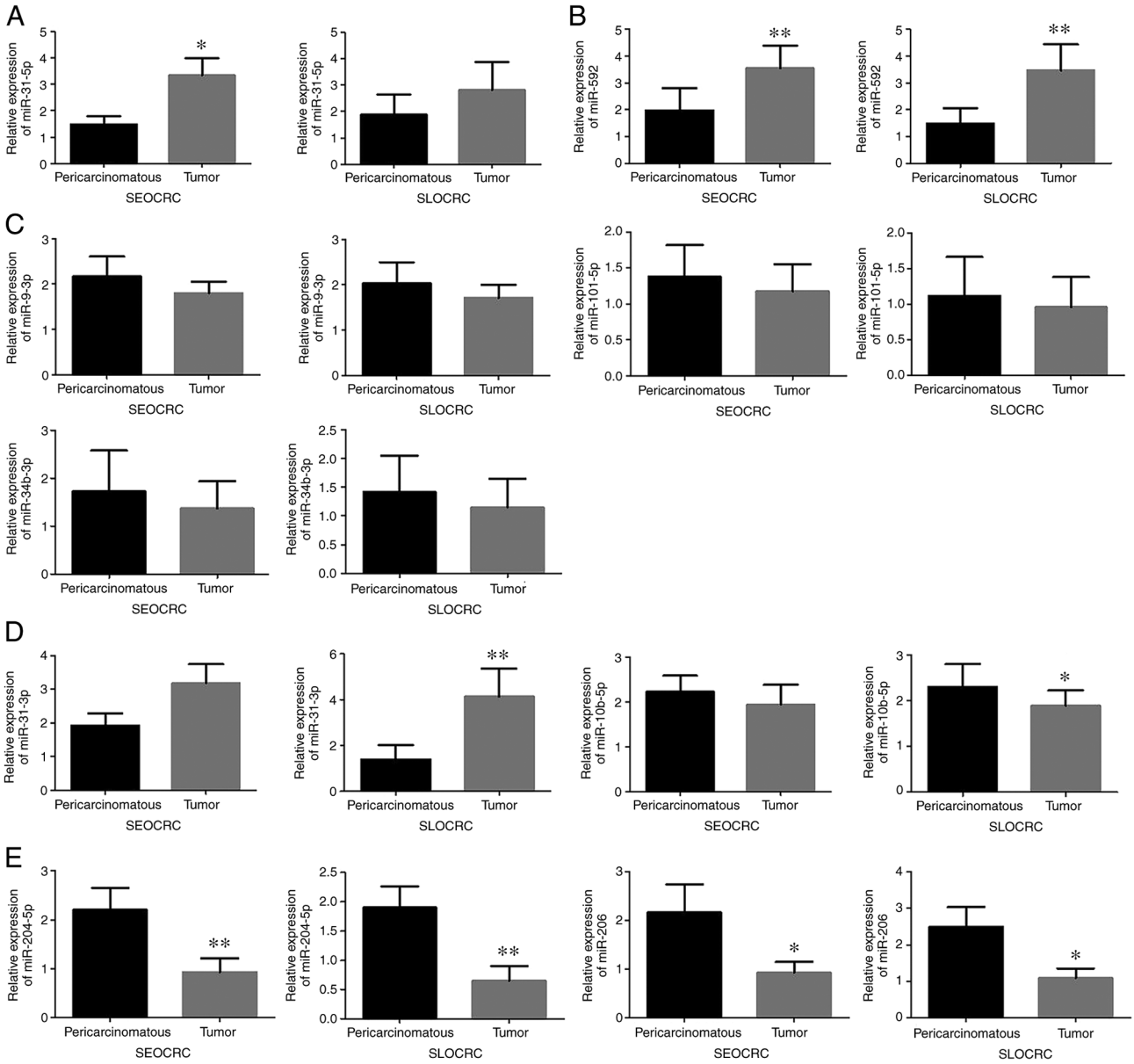

Figure 3. Expression levels of nine candidate miRNAs in tumor and paracancerous tissue samples from patients with SEOCRC or SLOCRC. (A) miR-31-5p level was significantly increased in tumor (n=13) compared with paracancerous tissue (n=13) in patients with SEOCRC (P=0.020). There were no significant differences between the tumor (n=11) and paracancerous tissue (n=11) in the SLOCRC group. (B) miR-592 levels were significantly increased in tumor compared with paracancerous tissue samples in both the SEOCRC (P<0.001) and the SLOCRC group (P=0.003). (C) No statistically significant difference was observed in the levels of miR-9-3p, miR-34b-3p and miR-101-5p between tumor and paracancerous tissue samples in either the SEOCRC group or the SLOCRC group. (D) No statistically significant difference was observed in the levels of miR-31-3p and miR-10b-5p between tumor and paracancerous tissue samples in the SEOCRC group. The level of miR-31-3p was significantly increased in tumor compared with paracancerous tissue samples in the SLOCRC group (P=0.002), while the level of miR-10b-5p was significantly decreased in tumor compared with paracancerous tissue samples in the SLOCRC group (P=0.042). (E) miR-204-5p and miR-206 levels were significantly downregulated in tumor compared with paracancerous tissue samples in both the SEOCRC (P<0.001 and P=0.049, respectively) and the SLOCRC group (P=0.001 and P=0.031, respectively). The data were obtained from Cohort 3. *P<0.05, **P<0.01. SEOCRC, sporadic early-onset colorectal cancer; SLOCRC, sporadic late-onset colorectal cancer.

the experimental group and TCGA groups (Table V) (22-31). Therefore, the miR-31-5p-*DMD* pair was selected as a candidate biomarker in the development of SEOCRC.

miR-31-5p acts as biomarker in patients with SEOCRC. To validate the expression of these nine miRNAs in patients with CRC, miRNA levels were determined using RT-q PCR in 13 tumor and 13 paracancerous tissue samples from patients with SEOCRC, and 11 tumor and 11 paracancerous tissue samples from patients with SLOCRC (Cohort 3). As shown in Fig. 3, the levels of miR-31-5p were significantly upregulated in tumor tissues compared with paracancerous tissues in patients with SEOCRC (P=0.020), whereas no significant difference was observed in the SLOCRC group (P=0.465; Fig. 3A). The level of miR-592 was significantly increased in tumor compared with paracancerous tissue samples in both the SEOCRC (P<0.001) and the SLOCRC group (P=0.003; Fig. 3B). No statistically significant difference was observed in the levels of miR-9-3p, miR-34b-3p and miR-101-5p between tumor and paracancerous tissue samples

Table VI. Association between DMD expression in sporadic colorectal cancer tissue with different clinicopathological features

Clinicopathological characteristics	DMD expression, n (%)		P-value
	Low (n=40) (%)	High (n=40) (%)	
Sex			0.259
Male	26 (65.0)	21 (52.5)	
Female	14 (35.0)	19 (47.5)	
Tumor size, cm			0.182
<5	18 (45.0)	24 (60.0)	
≥5	22 (55.0)	16 (40.0)	
Histological grade			0.052
Good or moderate	24 (60.0)	32 (80.0)	
Poor	16 (40.0)	8 (20.0)	
TNM stage			0.007[a]
II	17 (42.5)	29 (72.5)	
III	23 (57.5)	11 (27.5)	
Lymph node metastasis			
Yes	25 (62.5)	13 (32.5)	0.008[a]
No	15 (37.5)	27 (67.5)	

[a]P<0.01. The data were obtained from Cohort 3. DMD, dystrophin.

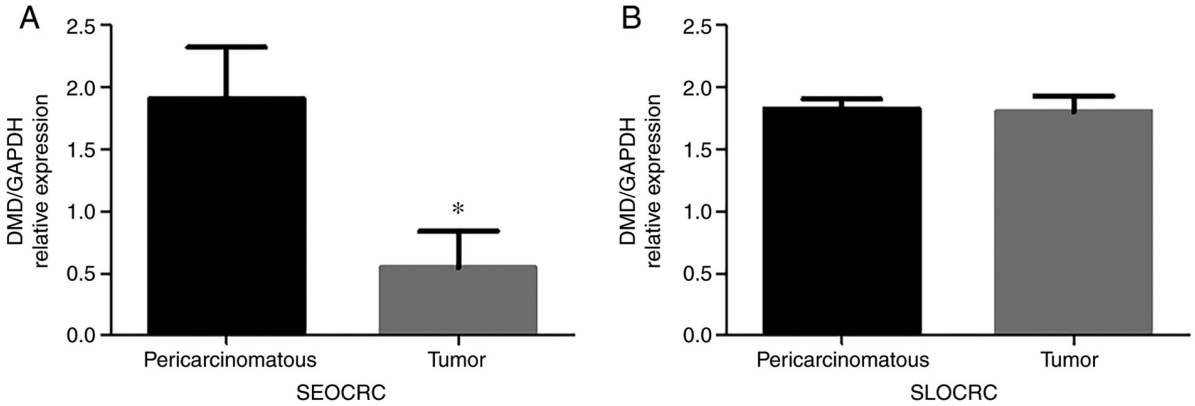

Figure 4. Expression of DMD in SEOCRC and SLOCRC. (A) DMD expression was significantly downregulated in tumor (n=13) compared with pericarcinomatous tissue samples (n=13) from patients with SEOCRC (P=0.040). (B) No statistical difference in expression of DMD between tumor (n=11) and pericarcinomatous tissue (n=11) in SLOCRC (P=0.896). The data were obtained from Cohort 3. *P<0.05. SEOCRC, sporadic early-onset colorectal cancer; SLOCRC, sporadic late-onset colorectal cancer; DMD, dystrophin.

in either the SEOCRC group (P=0.376, P=0.787 and P=0.138, respectively) or the SLOCRC group (P=0.276, P=0.131 and P=0.765, respectively; Fig. 3C). No statistically significant difference was observed in the levels of miR-31-3p and miR-10b-5p between tumor and paracancerous tissue samples in the SEOCRC group (P=0.058 and P=0.132). The level of miR-31-3p was significantly increased in tumor compared with paracancerous tissue samples in the SLOCRC group (P=0.002). However, the level of miR-10b-5p was significantly decreased in tumor compared with paracancerous tissue samples in the SLOCRC group (P=0.042) (Fig. 3D). By contrast, the levels of miR-204-5p and miR-206 were significantly downregulated in tumor compared with paracancerous tissue samples in both the SEOCRC (P<0.001 and P=0.049, respectively) and the SLOCRC group (P=0.001 and P=0.031, respectively; Fig. 3E).

DMD is downregulated in patients with SEOCRC. In order to verify the expression levels of *DMD* in SEOCRC, RT-qPCR was performed in 13 tumor and 13 paracancerous tissue samples from patients with SEOCRC, as well as 11 tumor tissues and 11 paracancerous tissue samples from patients with SLOCRC (cohort 3). The results demonstrated that the expression of *DMD* was downregulated in tumor tissue compared with paracancerous tissue samples of SEOCRC (P=0.040; Fig. 4A). However, there was no significant difference in *DMD* gene expression between cancer and paracancerous tissue of patients with SLOCRC (P=0.896; Fig. 4B).

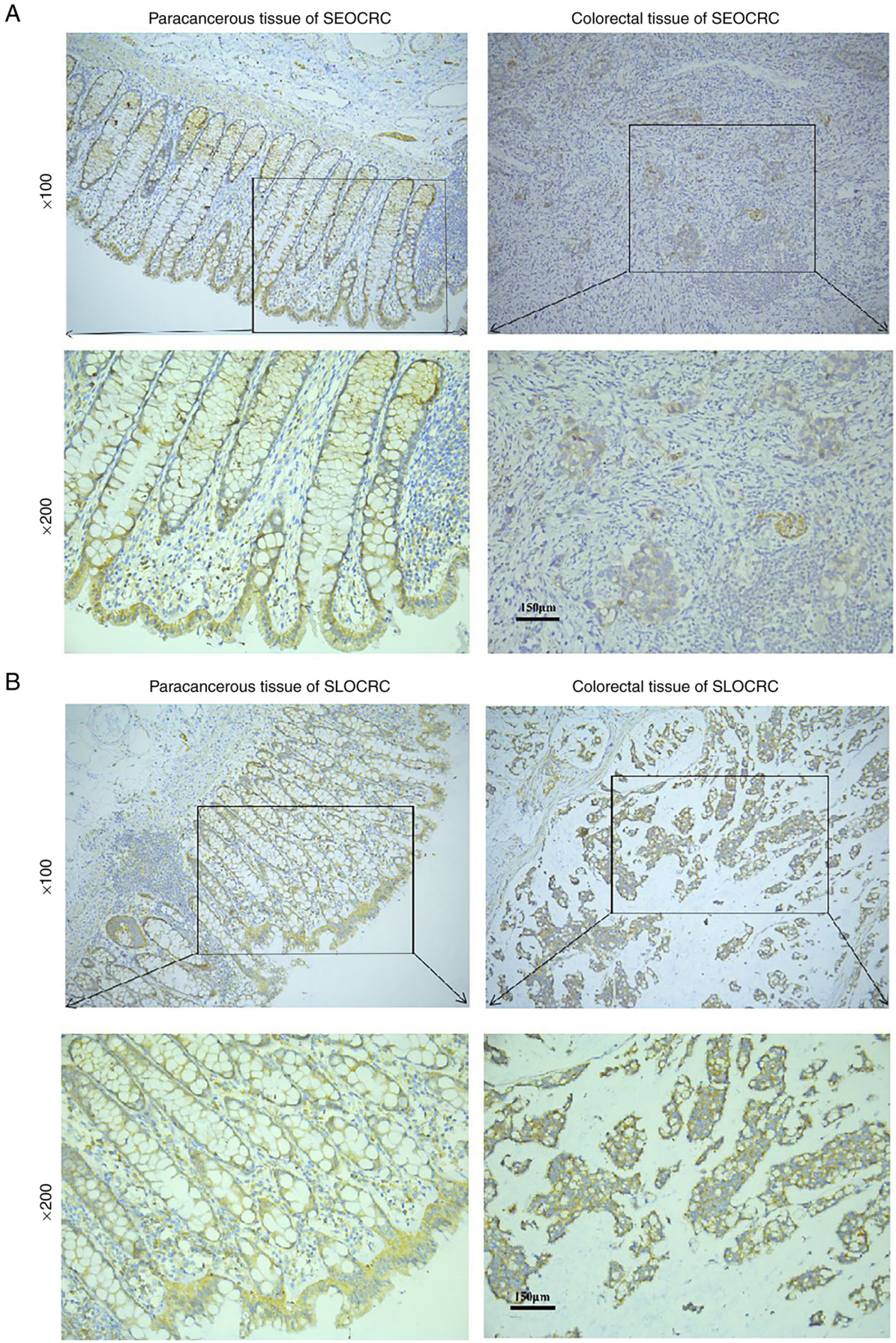

Figure 5. Protein expression of DMD in SEOCRC and SLOCRC. (A) *In situ* expression of DMD was observed in paracancerous epithelia but was faint in colorectal cancer cells in SEOCRC by immunostaining. (B) *In situ* expression of DMD was observed in paracancerous epithelia and colorectal cancer cells in SLOCRC by immunostaining. The data were obtained from Cohort 3. SEOCRC, sporadic early-onset colorectal cancer; SLOCRC, sporadic late-onset colorectal cancer.

Consistent with the aforementioned results, the expression of DMD at the protein level was also assessed using IHC staining in 13 paired tumor tissues and paracancerous tissues of SEOCRC, and 11 paired tumor tissues and paracancerous tissues of SLOCRC, respectively. As shown in Fig. 5, DMD protein expression was markedly decreased in tumor tissues compared with that in paired paracancerous tissue samples from patients with SEOCRC. However, there was no difference between tumors and paired paracancerous tissues of SLOCRC with respect to DMD expression. Collectively, these results indicate that a decrease of DMD may be associated with the development of SEOCRC.

Correlation of DMD expression with clinicopathological features of SEOCRC. In order to evaluate the association between *DMD* expression and clinicopathological variables, 80 patients with SEOCRC (cohort 4) were divided into a high-expression and a low-expression group (n=40 in each group) according to the median value of *DMD* expression. The correlation between *DMD* expression and clinicopathological features was assessed. As shown in Table VI, low expression of *DMD* was significantly associated with advanced pathological stage and increased incidence of lymph node metastasis (P=0.007 and P=0.008, respectively). However, no significant associations between *DMD* and other patient characteristics were observed. Moreover, the patients with low *DMD* expression had a significantly poorer prognosis than those with high *DMD* expression level in overall survival (P=0.011; Fig. 6A), cancer-specific survival (P=0.009; Fig. 6B) and recurrence free survival (P=0.014; Fig. 6C) in a Kaplan-Meier survival analysis.

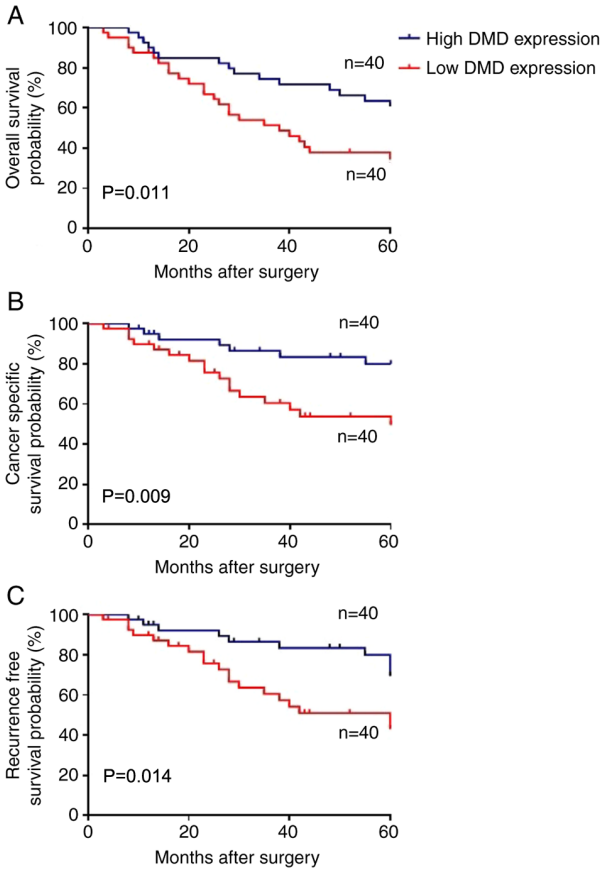

Figure 6. Kaplan-Meier survival curves of patients with sporadic early-onset colorectal cancer stratified according to DMD expression. (A) Patients with low expression had significantly poorer overall survival than those with high expression (P=0.011). (B) Patients with low expression had significantly poorer cancer specific survival than those with high expression (P=0.009). (C) Patients with low expression had significantly poorer recurrence free survival than those with high expression (P=0.014). The data were obtained from Cohort 4. DMD, dystrophin.

Discussion

Currently, the incidence of SEOCRC is increasing worldwide. Although the pathogenesis has been studied intensively, it still remains unclear. It has been recognized that the origin of the disease may be attributed to the presence of a large number of common, low-penetrance genetic variants, each exerting a small influence on risk (9). Accumulating evidence has also shown that 80% of sporadic EOCRCs tend to be microsatellite-stable and do not feature the CpG island methylator phenotype (32). In a study involving 18,218 clinical specimens, the alterations of *TP53* and *CTNNB1* were found to be more common in younger patients (<40) in the microsatellite-stable group, while *APC, KRAS, BRAF* and *FAM123B* were more frequently altered in older patients (≥50) with CRC. In the MSI-high cohort, the majority of genes have been proven to have a similar rate of alterations in all age group, but with significant differences in *APC, BRAF*, and *KRAS* (33). However, the younger group of this study included inherited and sporadic CRC. Additionally, another study has also identified ten candidate heterozygous variants (*BMPR1A, BRIP1, SRC, CLSPN, SEC24B, SSH2, ACACA, NR2C2, INPP4A*, and *DIDO1*) and five possibly biallelic autosomal recessive candidate genes (*ATP10B, PKHD1, UGGT2, MYH13, TFF3*) through exome sequencing in 51 early-onset non-familial CRC cases (34).

In the present study, the role of key genes and their regulatory miRNAs were examined in the development of SEOCRC by NGS and bioinformatics. Clinical samples (cohort 1) and TCGA (cohort 2) datasets were examined and it was demonstrated that the miR-31-5p-*DMD* axis was altered in SEOCRC in both cohorts. The expression of miR-31-5p was upregulated whereas *DMD* was downregulated in SEOCRC, which were further verified by qPCR and IHC. Therefore, the miR-31-5p-*DMD* axis may serve as a novel potential biomarker in the pathogenesis of SEOCRC.

miR-31-5p has been proposed as novel biomarker for the diagnosis and treatment of many types of cancer including oral cancer, renal cell carcinoma, CRC, nasopharyngeal carcinoma, and hepatocellular carcinoma (35-39). miR-31 plays an intricate role in human cancer function as onco-miR and tumor suppressor miR (19). Moreover, it can influence the drug sensitivity and efficacy of chemotherapy in colorectal cancer and hepatocellular carcinoma cells (18,39). It has been considered as a target of long noncoding or circular RNA in cardiomyocyte hypertrophy and pre-eclampsia (40,41), and a shared regulator of chronic mucus hypersecretion in asthma and chronic obstructive pulmonary disease (42). In the present study, miR-31 was upregulated in SEOCRC and DMD was downregulated.

The *DMD* gene encodes the dystrophin protein which forms a component of the dystrophin-glycoprotein complex

(DGC) bridging the inner cytoskeleton and the extracellular matrix. Deletion, duplication, and point mutation of *DMD* gene may cause Duchenne's muscular dystrophy, Becker muscular dystrophy (BMD), or cardiomyopathy (43-45). Altered *DMD* expression is also linked to the onset and progression of cancer, including myogenic tumors and even non-myogenic tumors (46-49), and it is considered as a new regulatory factor in tumor development and a new prognostic factor for tumor progression and survival. However, the molecular mechanism of *DMD* disorder in cancer is not clear, and the relationship between *DMD* gene and CRC has not been reported. In the present study, *DMD* was found to be downregulated in patients with SEOCRC and associated with tumor stage, lymph node metastasis and patient survival.

In summary, the present findings reveal a reduction of DMD and an increase of miR-31-5p in SEOCRC, suggesting that the miR-31-5p-*DMD* axis may contribute to the occurrence of SEOCRC and may serve as a new biomarker in the diagnosis and treatment of SEOCRC.

Acknowledgements

The authors would like to thank Dr Lijin Feng (Pathology Department, Shanghai Tenth People's Hospital of Tongji university) for his help in interpreting pathology and providing help in immunohistochemical experiments.

Funding

This study was supported by the Natural Science Foundation of Shanghai Tenth People's Hospital (No. 01.02.13.058).

Availability of data and materials

The datasets used and/or analyzed during the current study are available from the corresponding author on reasonable request. The NGS data generated and/or analyzed during the current study are available in the Sequence Read Archive (https://www.ncbi.nlm.nih.gov/sra/PRJNA787417) under BioProject no. PRJNA787417.

Authors' contributions

CL and ZL designed the study and were major contributors in writing the manuscript. CL, RW and WC collected the samples. CL, WC, WW and RW performed the NGS, PCR, IHC and analyzed and interpreted the data. XS and HW analyzed and interpreted the data, contributed to critical revisions on the intellectual content and revised the manuscript. All authors read and approved the final manuscript. CL and RW confirm the authenticity of all the raw data.

Ethics approval and consent to participate

All procedures performed in studies involving human participants were in accordance with the ethical standards of the institutional and national research committee and with the 1964 Declaration of Helsinki and its later amendments or comparable ethical standards. The study was approved by the ethics committee of The Shanghai Tenth People's Hospital affiliated to Tongji University (approval no. 2016-68). All patients provided written informed consent.

Patient consent for publication

Not applicable.

Competing interests

The authors declare that they have no competing interests.

References

1. Bray F, Ferlay J, Soerjomataram I, Siegel RL, Torre LA and Jemal A: Global cancer statistics 2018: GLOBOCAN estimates of incidence and mortality worldwide for 36 cancers in 185 countries. CA Cancer J Clin 68: 394-424, 2018.
2. Jayasekara H, English DR, Haydon A, Hodge AM, Lynch BM, Rosty C, Williamson EJ, Clendenning M, Southey MC, Jenkins MA, *et al*: Associations of alcohol intake, smoking, physical activity and obesity with survival following colorectal cancer diagnosis by stage, anatomic site and tumor molecular subtype. Int J Cancer 142: 238-250, 2018.
3. Mármol I, Sánchez-de-Diego C, Pradilla Dieste A, Cerrada E and Rodriguez Yoldi MJ: Colorectal carcinoma: A general overview and future perspectives in colorectal cancer. Int J Mol Sci 18: 197, 2017.
4. Loomans-Kropp HA and Umar A: Increasing incidence of colorectal cancer in young adults. J Cancer Epidemiol 2019: 9841295, 2019.
5. Patel SG and Ahnen DJ: Colorectal cancer in the young. Curr Gastroenterol Rep 20: 15, 2018.
6. Yeo H, Betel D, Abelson JS, Zheng XE, Yantiss R and Shah MA: Early-onset colorectal cancer is distinct from traditional colorectal cancer. Clin Colorectal Cancer 16: 293-299.e6, 2017.
7. Burnett-Hartman AN, Powers JD, Chubak J, Corley DA, Ghai NR, McMullen CK, Pawloski PA, Sterrett AT and Feigelson HS: Treatment patterns and survival differ between early-onset and late-onset colorectal cancer patients: The patient outcomes to advance learning network. Cancer Causes Control 30: 747-755, 2019.
8. Strum WB and Boland CR: Clinical and genetic characteristics of colorectal cancer in persons under 50 years of age: A review. Dig Dis Sci 64: 3059-3065, 2019.
9. Stigliano V, Sanchez-Mete L, Martayan A and Anti M: Early-onset colorectal cancer: A sporadic or inherited disease? World J Gastroenterol 20: 12420-12430, 2014.
10. Pearlman R, Frankel WL, Swanson B, Zhao W, Yilmaz A, Miller K, Bacher J, Bigley C, Nelsen L, Goodfellow PJ, *et al*: Prevalence and spectrum of germline cancer susceptibility gene mutations among patients with early-onset colorectal cancer. JAMA Oncol 3: 464-471, 2017.
11. Mo X, Su Z, Yang B, Zeng Z, Lei S and Qiao H: Identification of key genes involved in the development and progression of early-onset colorectal cancer by co-expression network analysis. Oncol Lett 19: 177-186, 2020.
12. Pertea M, Kim D, Pertea GM, Leek JT and Salzberg SL: Transcript-level expression analysis of RNA-seq experiments with HISAT, StringTie and Ballgown. Nat Protoc 11: 1650-1667, 2016.
13. Robinson MD, McCarthy DJ and Smyth GK: edgeR: A bioconductor package for differential expression analysis of digital gene expression data. Bioinformatics 26: 139-140, 2010.
14. Benjamini Y: Discovering the false discovery rate. J R Stat Soc B 72: 405-416 2010.
15. Livak KJ and Schmittgen TD: Analysis of relative gene expression data using real-time quantitative PCR and the 2(-Delta Delta C(T)) method. Methods 25: 402-408, 2001.
16. Gu S, Lin S, Ye D, Qian S, Jiang D, Zhang X, Li Q, Yang J, Ying X, Li Z, *et al*: Genome-wide methylation profiling identified novel differentially hypermethylated biomarker MPPED2 in colorectal cancer. Clin Epigenetics 11: 41, 2019.
17. Kubota N, Taniguchi F, Nyuya A, Umeda Y, Mori Y, Fujiwara T, Tanioka H, Tsuruta A, Yamaguchi Y and Nagasaka T: Upregulation of microRNA-31 is associated with poor prognosis in patients with advanced colorectal cancer. Oncol Lett 19: 2685-2694, 2020.

18. Ren TJ, Liu C, Hou JF and Shan FX: CircDDX17 reduces 5-fluorouracil resistance and hinders tumorigenesis in colorectal cancer by regulating miR-31-5p/KANK1 axis. Eur Rev Med Pharmacol Sci 24: 1743-1754, 2020.
19. Sur D, Cainap C, Burz C, Havasi A, Chis IC, Vlad C, Milosevic V, Balacescu O and Irimie A: The role of miRNA-31-3p and miR-31-5p in the anti-EGFR treatment efficacy of wild-type K-RAS metastatic colorectal cancer. Is it really the next best thing in miRNAs? J BUON 24: 1739-1746, 2019.
20. Hsu HH, Kuo WW, Shih HN, Cheng SF, Yang CK, Chen MC, Tu CC, Viswanadha VP, Liao PH and Huang CY: FOXC1 regulation of miR-31-5p confers oxaliplatin resistance by targeting LATS2 in colorectal cancer. Cancers (Basel) 11: 1576, 2019.
21. De Robertis M, Mazza T, Fusilli C, Loiacono L, Poeta ML, Sanchez M, Massi E, Lamorte G, Diodoro MG, Pescarmona E, *et al*: EphB2 stem-related and EphA2 progression-related miRNA-based networks in progressive stages of CRC evolution: Clinical significance and potential miRNA drivers. Mol Cancer 17: 169, 2018.
22. Cacchiarelli D, Incitti T, Martone J, Cesana M, Cazzella V, Santini T, Sthandier O and Bozzoni I: miR-31 modulates dystrophin expression: New implications for Duchenne muscular dystrophy therapy. EMBO Rep 12: 136-141, 2011.
23. Koumangoye RB, Andl T, Taubenslag KJ, Zilberman ST, Taylor CJ, Loomans HA and Andl CD: SOX4 interacts with EZH2 and HDAC3 to suppress microRNA-31 in invasive esophageal cancer cells. Mol Cancer 14: 24, 2015.
24. Suzuki H, Yamamoto E, Nojima M, Kai M, Yamano HO, Yoshikawa K, Kimura T, Kudo T, Harada E, Sugai T, *et al*: Methylation-associated silencing of microRNA-34b/c in gastric cancer and its involvement in an epigenetic field defect. Carcinogenesis 31: 2066-2073, 2010.
25. Gabriely G, Yi M, Narayan RS, Niers JM, Wurdinger T, Imitola J, Ligon KL, Kesari S, Esau C, Stephens RM, *et al*: Human glioma growth is controlled by microRNA-10b. Cancer Res 71: 3563-3572, 2011.
26. Geekiyanage H and Galanis E: MiR-31 and miR-128 regulates poliovirus receptor-related 4 mediated measles virus infectivity in tumors. Mol Oncol 10: 1387-1403, 2016.
27. Chen PH, Chang CK, Shih CM, Cheng CH, Lin CW, Lee CC, Liu AJ, Ho KH and Chen KC: The miR-204-3p-targeted IGFBP2 pathway is involved in xanthohumol-induced glioma cell apoptotic death. Neuropharmacology 110: 362-375, 2016.
28. Sim SE, Lim CS, Kim JI, Seo D, Chun H, Yu NK, Lee J, Kang SJ, Ko HG, Choi JH, *et al*: The brain-enriched MicroRNA miR-9-3p regulates synaptic plasticity and memory. J Neurosci 36: 8641-8652, 2016.
29. Zhang YJ, Xu F, Zhang YJ, Li HB, Han JC and Li L: miR-206 inhibits non small cell lung cancer cell proliferation and invasion by targeting SOX9. Int J Clin Exp Med 8: 9107-9113, 2015.
30. Liu N, Zhang L, Wang Z, Cheng Y, Zhang P, Wang X, Wen W, Yang H, Liu H and Jin W: MicroRNA-101 inhibits proliferation, migration and invasion of human glioblastoma by targeting SOX9. Oncotarget 8: 19244-19254, 2017.
31. Zhu Q, Gong L, Wang J, Tu Q, Yao L, Zhang JR, Han XJ, Zhu SJ, Wang SM, Li YH, *et al*: miR-10b exerts oncogenic activity in human hepatocellular carcinoma cells by targeting expression of CUB and sushi multiple domains 1 (CSMD1). BMC Cancer 16: 806, 2016.
32. Cavestro GM, Mannucci A, Zuppardo RA, Di Leo M, Stoffel E and Tonon G: Early onset sporadic colorectal cancer: Worrisome trends and oncogenic features. Dig Liver Dis 50: 521-532, 2018.
33. Lieu CH, Golemis EA, Serebriiskii IG, Newberg J, Hemmerich A, Connelly C, Messersmith WA, Eng C, Eckhardt SG, Frampton G, *et al*: Comprehensive genomic landscapes in early and later onset colorectal cancer. Clin Cancer Res 25: 5852-5858, 2019.
34. Thutkawkorapin J, Lindblom A and Tham E: Exome sequencing in 51 early onset non-familial CRC cases. Mol Genet Genomic Med 7: e605, 2019.
35. Lu Z, He Q, Liang J, Li W, Su Q, Chen Z, Wan Q, Zhou X, Cao L, Sun J, *et al*: miR-31-5p is a potential circulating biomarker and therapeutic target for oral cancer. Mol Ther Nucleic Acids 16: 471-480, 2019.
36. Li Y, Quan J, Chen F, Pan X, Zhuang C, Xiong T, Zhuang C, Li J, Huang X, Ye J, *et al*: MiR-31-5p acts as a tumor suppressor in renal cell carcinoma by targeting cyclin-dependent kinase 1 (CDK1). Biomed Pharmacother 111: 517-526, 2019.
37. Peng H, Wang L, Su Q, Yi K, Du J and Wang Z: MiR-31-5p promotes the cell growth, migration and invasion of colorectal cancer cells by targeting NUMB. Biomed Pharmacother 109: 208-216, 2019.
38. Yi SJ, Liu P, Chen BL, Ou-Yang L, Xiong WM and Su JP: Circulating miR-31-5p may be a potential diagnostic biomarker in nasopharyngeal carcinoma. Neoplasma 66: 825-829, 2019.
39. Chen Y, Zhao H, Li H, Feng X, Tang H, Qiu C, Zhang J and Fu B: LINC01234/MicroRNA-31-5p/MAGEA3 axis mediates the proliferation and chemoresistance of hepatocellular carcinoma cells. Mol Ther Nucleic Acids 19: 168-178, 2020.
40. Li H, Shi H, Zhang F, Xue H, Wang L, Tian J, Xu J and Han Q: LncRNA Tincr regulates PKCε expression in a miR-31-5p-dependent manner in cardiomyocyte hypertrophy. Naunyn Schmiedebergs Arch Pharmacol 393: 2495-2506, 2020.
41. Li W, Yu N, Fan L, Chen SH and Wu JL: Circ_0063517 acts as ceRNA, targeting the miR-31-5p-ETBR axis to regulate angiogenesis of vascular endothelial cells in preeclampsia. Life Sci 244: 117306, 2020.
42. Tasena H, Boudewijn IM, Faiz A, Timens W, Hylkema MN, Berg M, Ten Hacken NHT, Brandsma CA, Heijink IH and van den Berge M: MiR-31-5p: A shared regulator of chronic mucus hypersecretion in asthma and chronic obstructive pulmonary disease. Allergy 75: 703-706, 2020.
43. Chamberlain JR and Chamberlain JS: Progress toward gene therapy for duchenne muscular dystrophy. Mol Ther 25: 1125-1131, 2017.
44. Okubo M, Noguchi S, Hayashi S, Nakamura H, Komaki H, Matsuo M and Nishino I: Exon skipping induced by nonsense/frameshift mutations in DMD gene results in Becker muscular dystrophy. Hum Genet 139: 247-255, 2020.
45. Kamdar F and Garry DJ: Dystrophin-deficient cardiomyopathy. J Am Coll Cardiol 67: 2533-2546, 2016.
46. Luce LN, Abbate M, Cotignola J and Giliberto F: Non-myogenic tumors display altered expression of dystrophin (DMD) and a high frequency of genetic alterations. Oncotarget 8: 145-155, 2017.
47. Juratli TA, McCabe D, Nayyar N, Williams EA, Silverman IM, Tummala SS, Fink AL, Baig A, Martinez-Lage M, Selig MK, *et al*: DMD genomic deletions characterize a subset of progressive/higher-grade meningiomas with poor outcome. Acta Neuropathol 136: 779-792, 2018.
48. Mauduit O, Delcroix V, Lesluyes T, Pérot G, Lagarde P, Lartigue L, Blay JY and Chibon F: Recurrent DMD deletions highlight specific role of Dp71 isoform in soft-tissue sarcomas. Cancers (Basel) 11: 922, 2019.
49. Saba KH, Cornmark L, Rissler M, Fioretos T, Åström K, Haglund F, Rosenberg AE, Brosjö O and Nord KH: Genetic profiling of a chondroblastoma-like osteosarcoma/malignant phosphaturic mesenchymal tumor of bone reveals a homozygous deletion of CDKN2A, intragenic deletion of DMD, and a targetable FN1-FGFR1 gene fusion. Genes Chromosomes Cancer 58: 731-736, 2019.

This work is licensed under a Creative Commons Attribution-NonCommercial-NoDerivatives 4.0 International (CC BY-NC-ND 4.0) License.